Heliyon 9 (2023) e15554

Contents lists available at ScienceDirect

Heliyon

journal homepage: www.cell.com/heliyon

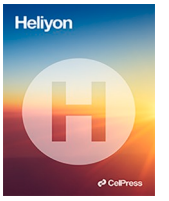

Research article

Drying kinetics and attributes of fructus aurantii processed by hot air thin-layer drying at different temperatures

Tingting Bai [a,b], Quan Wan [a,b], XiangBao Liu [c], Rui Ke [d], Yating Xie [a], Tao Zhang [a], Min Huang [a], Jinlian Zhang [a,*]

[a] *Jiangxi University of Chinese Medicine, China*
[b] *Affiliated Hospital of Inner Mongolia University for Nationalities, China*
[c] *Jiangxi Tongshantang Chinese Medicine Beverage Co., China*
[d] *Jiangxi Jingde Chinese Medicine Co., China*

ARTICLE INFO

Keywords:
Fructus aurantii
Drying kinetics
Aroma components
Hot air thin-layer drying
Electronic nose technology

ABSTRACT

The primary objectives of this study were to evaluate the drying kinetics of Fructus Aurantii (FA), and to investigate how hot air drying at various temperatures affected the surface texture and sensory quality of the volatile fragrance components. The results were best simulated by the Overhults model, and use of scanning electron microscopy (SEM) and Heracles Neo ultra-fast gas phase electronic nose technology allowed for detection of changes in surface roughness and aromatic odors. The limonene content varied from 74.1% to 84.2% depending on the drying temperature, which ranged from 35°C to 75 °C. Furthermore, principal component analysis (PCA) revealed that the aromatic compound profile underwent considerable changes during the drying process. Overall, the present findings demonstrate that hot air thin-layer drying at 55 °C can significantly enhance the final quality of FA while preserving the taste properties and providing optimum medicinal and culinary characteristics.

1. Introduction

Fructus Aurantii (FA) is the dried unripe fruit of *Citrus aurantium* Linn, a member of the Rutaceae family, and its cultivated variants. It is often used as a medication in clinical therapy and has the benefits of regulating Qi, resolving stagnation, and removing distention [1]. Contemporary studies have demonstrated that the essential chemical components of FA include its volatile oil, as well as flavonoids and alkaloids. The volatile oil largely consists of monoterpenes, sesquiterpenes, and aliphatic compounds, with its primary constituents being limonene, α-terpinene, and linalool [2]. A portion of the volatile oil in the mixture can be removed from medicinal preparations to lessen the severely harmful consequences to vital energy, which include effects such as stagnation, cough suppression, expectoration [3], and stagnation [4].

A variety of volatile components are abundant in FA, but it is prone to rapid loss of active chemicals due to its high temperature sensitivity. These biological and sensory aspects are, however, crucial in determining the overall quality of the plant material [5]. Where artificial drying processes are used, the mechanism of associated quality deterioration is currently unclear, resulting in irrationally designed drying procedures and making it difficult to determine the point at which drying is optimally complete. Thus, issues of "under-drying" or "over-drying" are a constant problem. Excessive drying and higher temperatures cause color degradation, volatile

* Corresponding author.
E-mail address: jxjzzjl@163.com (J. Zhang).

https://doi.org/10.1016/j.heliyon.2023.e15554
Received 16 October 2022; Received in revised form 6 April 2023; Accepted 13 April 2023
Available online 17 April 2023

oil loss, and active component degradation [6–8]. Too much drying can cause the herb's moisture content to fall short of pharmacopeia guidelines, making it susceptible to mold growth and biodegradation [9]. In turn, this might lead to loss of taste diversity and therapeutic efficacy, lowering the quality of aromatic herbal drinks made using FA [10]. The quality of these drinks is therefore directly impacted by the drying step, which is a crucial but presently inconsistent stage during the processing of aromatic herbs.

Due to its practicality, low cost, and proven effectiveness, hot air drying [11]is typically regarded as the ideal technique for drying plant-derived food components. Compared with drying in the sun or in the shade, it offers the advantages of controlled temperature and weather resilience. The plant material is spread out in suitable equipment in thin layers, with a rapid flow of heated air traveling through each layer, resulting in significantly increased drying efficiency. For therapeutic herbs, this can assure better medicinal quality [12]. In this work, the link between moisture ratio and drying time for FA was fit and validated using empirical models such as the Midilli, Page, and Overhults models. In the processing of FA, we were able to improve quality control and optimize the drying process at source by utilizing the Heracles Neo ultra-fast gas-phase electronic nose [13] to identify changes in volatile components.

2. Materials and methods

2.1. Materials

A sample of FA was purchased from Nanchang, Jiangxi Province, China, and confirmed by Prof. Shouwen Zhang (Jiangxi University of Chinese Medicine) as the dried immature fruit of *C. aurantium* L., family Rutaceae.

2.2. Hot air thin-layer drying of FA

In a forced air oven (BPG-9070A, 1500 W, Yiheng Inc., Shanghai, China), 100 g batches of processed FA were dried at 35, 45, 55, 65, and 75 °C. The FA samples were thinly layered in a single layer (2–3 cm thick) on a tray with a diameter of 15 cm. A built-in heater inside the oven wall produced heat, and airflow from natural convection was 2.0 m s^{-1}. Vents at the back of the oven (5 cm diameter) allowed the exhaust gas to escape. At intervals of 5 min (0–60 min run time), 10 min (60–180 min), 20 min (180–300 min), 30 min (300–420 min), and thereafter every 60 min, the tray was removed and weighed by electronic balance (FA2004A, Shanghai Precision Scientific Inc., China). Drying was continued until a constant weight was attained.

2.3. Microstructural analysis of dried FA

Scanning electron microscopy (SEM) was used to assess the effects of various treatments on the microstructure of dried samples. A thin coating of gold film was applied to the samples, which were mounted on double-sided tape. Imaging was then carried out using an FEI-Quanta250 instrument (Waltham, MA, USA) with an acceleration voltage of 15 kV.

2.4. Preparation of volatile extracts

The inner shell of FA was dug out using a knife, then it was washed to remove sediment, allowed to stand for 12 h, flattened with an iron anchor, cut into flat semicircles, and pressed on a wooden frame until the surface of the citrus was slightly white mold with white hyphae, then finally cut into 0.2 cm thick phoenix-eye pieces [14].

2.5. Determining the behavior of the hot air thin layer drying process

2.5.1. Determination of initial dry basis moisture content

The moisture content of FA was determined by using the drying method, then it was subjected to rapid moisture measurement with the temperature set at 105 °C until it was fully dried. The moisture content of the original sample was then calculated using the following formula (Eq. 1):

$$M = \frac{w_w - w_d}{W_d} \quad (1)$$

Where, M is the moisture content of FA, w_w is the wet weight of the sample, and W_d is the dry weight.

Table 1
Mathematical model equation for thin-layer drying.

Model Name	Model Equation	References
Logarithmic	$MR = a\exp(-kt)+c$	[34]
Lewis	$MR = \exp(-kt)$	[35]
Overhults	$MR = \exp[-(kt)^y]$	[36]
Henderson & Pabis	$MR = a\exp(-kt)$	[37]
Two terms Exponential	$MR = a\exp(-kt) + (1-a)\exp(-kat)$	[38]

Note:t = drying time , *a,k,b,y,c* = the model coefficient.

2.5.2. Mathematical model for drying kinetics of FA

To accurately explore the properties of dried FA, it was crucial to precisely characterize the drying behavior. In this study, drying of FA at various temperatures was evaluated using five empirical models (Table 1) by fitting the experimental drying data with each model. The dimensionless moisture ratio, MR, was calculated using Equation (2):

$$MR = \frac{M_t - M_e}{M_0 - M_e} \tag{2}$$

Where, M_0 is the initial moisture content of FA, M_t is the water content, and M_e denotes the equilibrium water content [15]. Since M_e is negligible relative to M_0 and M_t, Equation (2) may be therefore be reduced to Equation (3):

$$MR = \frac{M_t}{M_0} \tag{3}$$

To assess the goodness of fit, the statistical correlation coefficient R^2, chi-squared value χ^2, and root mean square error (RMSE) were utilized. In general, higher R^2, along with lower χ^2 and RMSE, indicate better outcomes for model fitting. Equations (4)–(6) were used to obtain these parameters, as indicated below [16].

$$R^2 = 1 - \frac{\sum_{i=1}^{n}\left(MR_{exp,i} - MR_{pre,i}\right)2}{\sum_{i=1}^{n}\left(MR_{exp,i} - MR_{pre,i}\right)2} \tag{4}$$

$$\chi^2 = \frac{\sum_{i=1}^{n}\left(MR_{exp,i} - MR_{pre,i}\right)2}{N - Z} \tag{5}$$

$$\mathrm{RMSE} = \sqrt{\frac{1}{N}\sum_{i=1}^{n}\left(MR_{exp,i} - MR_{pre,i}\right)^{\ 2}} \tag{6}$$

Where, $MR_{exp,i}$ and $MR_{pre,i}$ are the i-th moisture ratio measured during the drying experiment, N is the number of data points measured in the experiment, and Z is the number of factor levels.

2.6. Effective diffusion coefficient (D_{eff}) and activation energy (E_a)

2.6.1. Effective diffusion coefficient (D_{eff})

During the hot air drying process, internal moisture movement within FA is typically thought to occur via diffusion (liquid or vapor). It is therefore taken that the effective water diffusivity, D_{eff}, of moisture during the drying process of FA can be computed by integrating the experimental data over the entire analytical procedure, since the drying process was carried out under non-stationary conditions. Equation (7) was therefore used to determine D_{eff} from the FA drying experiments [16].

$$\mathrm{MR} = 8\pi^{-2}\sum_{i=1}^{n}(2\mathrm{n}+1)^{-2}\exp\left[-(2\mathrm{n}+1)^2\pi^2 D_{eff}\ tL_0^{-2}\right] \tag{7}$$

Where, L is the sample thickness (in m) of the thin layer of FA, n is the number of experimental samples, and t is the duration of the experiment. This equation may be used to assess whether a linear relationship exists between ln MR and time by taking the natural logarithm of each side (giving Equation (8), as shown below). Plotting the experimental drying data according to Eq. (8) usually yields the answer, and if the expected linear relationship between ln MR and drying time (t) is observed, D_{eff} may be derived from the slope of the line.

$$\ln\mathrm{MR} = \ln\left(8 / \pi^2\right) - \pi^2 D_{eff}\ t / L^2 \tag{8}$$

2.6.2. Activation energy (E_a)

The amount of energy needed to evaporate one unit of water during the drying process is referred to as the activation energy (E_a), and the higher the E_a of a material, the more challenging it is to dry. Assuming that the relationship between the temperature of the material and the diffusion of water within it follows the Arrhenius equation, the relationship between D_{eff} and E_a can be described according to Equation (9) [16]:

$$D_{eff} = D_0 \exp\left(-\frac{E_a}{RT}\right) \tag{9}$$

Where, D_{eff} is the effective water diffusivity ($m^2\ s^{-1}$), D_0 is the high-temperature infinite diffusivity ($m^2\ s^{-1}$), E_a denotes the activation energy (kJ mol^{-1}), R is the ideal gas constant (8.314 J mol^{-1} K^{-1}), and T is the absolute temperature (K). The activation energy may therefore be calculated by plotting ln D_{eff} against 1/T.

2.7. Heracles Neo ultra-fast gas-phase electronic nose analysis of volatile extracts from dried FA

The experimental samples were pulverized and sieved (using a No. 2 sieve), then wrapped in aluminum foil bags and refrigerated. For analysis, 1.0 g of material was weighed into a 20 mL headspace vial and sealed with an aluminum/silicone gasketed cap. In contrast to standard metal oxide semiconductor (MOS) electronic noses that rely on metal oxide sensors, the Heracles Neo Analyzer is a rapid gas-phase electronic nose with an inbuilt pre-concentration trap. To begin the analysis, each sample was first placed in an incubator to allow the volatile components to concentrate in the gas phase part of the headspace vial and reach equilibrium. The gaseous sample was fed into the pre-concentration trap and the trapped components were promptly released and separated into MXT-5 (10 m × 0.18 mm, 0.4 μm) and MXT-1701 (10 m × 0.18 mm, 0.4 μm) columns for detection by two post-column hydrogen flame ionization detectors (FIDs). Signals were recorded using Alpha Soft-17(Alpha Software, USA). Run parameters were as follows: incubator stirring speed 500 rpm (5 s working, 2 s pause); incubation temperature 75 °C; incubation time 10 min; sample amount 1.0 g; injection volume 4,000 μL; injection speed 125 L s^{-1}; trap temperature 40 °C; injection temperature 200 °C; injection duration 37 s; inlet temperature 200 °C. The programmed temperature gradient conditions were: initial furnace temperature 50 °C; ramp to 160 °C at 1.0 °C s^{-1}; hold for 0 s; ramp to 165 °C at 0.2 °C s^{-1}; hold for 5 s; ramp to 225 °C at 2.0 °C s^{-1} then to 250 °C over 30 s.

2.8. Statistical analysis

The experimental data were processed and analyzed using Microsoft Excel 2010 and Origin 2021b 64Bit. 64Bit. An external standard curve was used for quantitative analysis. The NIST 2014 mass spectral library was searched to identify the different volatile components. A multivariate statistical analysis of each sample's olfactory fingerprints was carried out using Alpha Soft 17.0 (Toulouse, France).

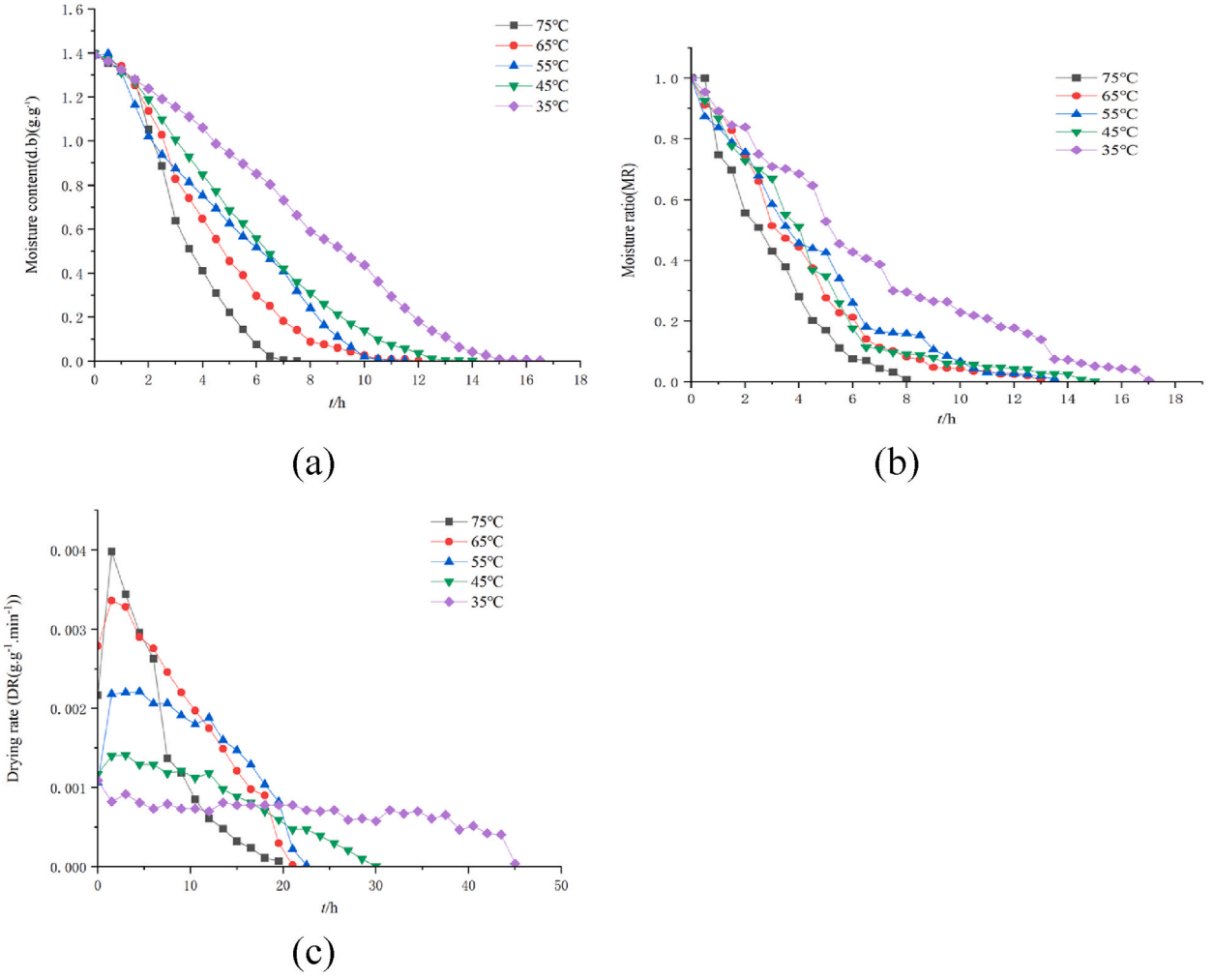

Fig. 1. Drying kinetic curve of Fructus aurantii. (a) dry basis moisture content of Fructus aurantii, (b) the moisture ratio curve of Fructus aurantii, (c) drying rate curves of Fructus aurantia at different drying temperature.

3. Results and discussion

3.1. Drying kinetics of FA

The original dry basis moisture content of FA was 1.45 ± 0.01 g g^{-1}. All experimental data, with the recorded mass of FA samples at various time points, were processed and analyzed using Origin 2021b 64Bit. in accordance with the corresponding formula, as described above. Fig. 1 shows the results for dry basis moisture content [denoted as moisture content (d.b)] versus time (h) during the drying process. The temporal variation of FA dry basis moisture content at different hot air drying temperatures is depicted in Fig. 1a. The value of [moisture content (d.b)] decreased continuously over time, with a more rapid drying rate in the early and middle stages that gradually decreased later, as can be seen from the slope of the curve. The drying process reached completion in a shorter amount of time with increasing temperature [17]. Drying durations were accurately calculated at 45 °C, 55 °C, and 65 °C, and were found to be 14 h, 12 h, and 11 h, respectively. The longest and shortest drying times were measured as 17.5 h (35 °C) and 8 h (75 °C). Thus, the temperature had a big influence on the time required for FA to dry. The variation of MR at different drying temperatures is also shown, along with the drying rate (Fig. 1b), confirming that the effect of air temperature correlates with drying rate when preparing dried FA samples.

Additionally, as seen in the graphs, the slope of the curve indicates a quick drying rate of FA in the early and middle phases that tended to gradually slow down in the latter stages (Fig. 1). Furthermore, moisture migration was accelerated with higher hot air temperature, resulting in relative drying rate increases [18]. When plotting the variation of drying rate (DR) over time (h), the slope of the drying curve initially rises during the early stages of the process (Fig. 1c). In addition, the initial drying rate is faster at higher temperatures and the drying process takes less time to complete. At 75 °C, there was a clear decreasing tendency in drying rate with time, and the lower the temperature, the flatter this downward trend proved to be. These results illustrate how important the influence of temperature is on FA drying rate. The situation arises because the material's internal and surface temperatures rise rapidly at the same time. This heating causes water on the surface to evaporate and disperse, leading to a lower surface temperature compared with the internal temperature, and creating an internal-to-external temperature gradient that drives moisture from the interior to the surface [19]. As a result, release of internal moisture quickens its dispersion to increase drying effectiveness [20]. The rapid drying (initial high drying rate) and deceleration periods are when moisture content is reduced the most. According to the literature, the second rule of thermodynamics—which states that water diffuses from the interior to the surface and travels from areas of higher to lower moisture content—might explain the delayed drying phase observed for *Hovenia* [21]. Nevertheless, the drying of various foodstuffs and agricultural goods relies on the primary physical processes of water migration and diffusion [22–24]. Our findings indicate that drying temperature adjustment can help shorten drying times, achieve high active ingredient retention, preserve color [25]. Further research is required, however, because the physicochemical, textural, and sensory qualities of materials can be gradually altered by changes in energy at various drying stages.

The drying kinetics of FA were further analyzed using the selected typical models in combination with the previously provided data (Table 1), and the resultant statistics are presented in Table 2 and Table 3. The R^2 of all models (1–5) at various drying temperatures was determined to be > 0.95. However, according to the derived statistics, model 3 (the Overhults model) had the greatest R^2 value as well as the lowest χ^2 and RMSE, suggesting that this model offered the best fit for the experimental data. Consequently, the Overhults model may be used to predict the drying behavior of FA. To confirm this, the performance of the Overhults model was evaluated by comparing the measured and predicted values of MR at various drying temperatures (Fig. 2a). As is evident, the experimental and modeled values were in close agreement, indicating that the Overhults model could successfully anticipate changes in MR throughout the drying process of FA, at temperatures of 35–75 °C.

Regression analysis of experimental ln MR for the cooling period, with the corresponding time points, allowed us to derive effective diffusion coefficients (D_{eff}) of 1.15×10^{-9} (35 °C), 2.22×10^{-9} (45 °C), 2.09×10^{-9} (55 °C), 2.70×10^{-9} (65 °C), and 2.09×10^{-9} (75 °C) m^2 s^{-1}. In addition, a linear relationship was seen between the natural logarithm of the effective diffusion coefficient (ln D_{eff}) and the inverse of temperature (1/T), as shown in Fig. 2b. This permitted the activation energy (E_a) of water diffusion during hot air drying of FA to be determined as 11.95 kJ mol^{-1}, which falls within the 10.4–28.1 kJ mol^{-1} range of E_a reported for drying of orange peel [26].

3.2. Effect of hot air thin-layer drying on FA textural properties

For food and pharmaceutical items, surface texture qualities are an important feature and a vital indicator of quality compliance.

Table 2
Model coefficients of the Overhults model at different drying temperature.

Temperature	Model Coeffcients	
	a	k
35 °C	1.29808	0.0771
45 °C	1.5248	0.0967
55 °C	1.32094	0.12348
65 °C	1.47672	0.11443
75 °C	1.36342	0.20126

Table 3
Statistical parameters for various models.

Model	SP	35 °C	45 °C	55 °C	65 °C	75 °C
1	R^2	0.990465	0.971786	0.988813	0.984217	0.990091
	X^2	0.000879	0.002930	0.001085	0.001689	0.0011
	RMSE	0.02923	0.053256	0.032353	0.040333	0.032172
2	R^2	0.970138	0.95377	0.970083	0.95046	0.963957
	X^2	0.002754	0.004803	0.002904	0.005363	0.004
	RMSE	0.051725	0.068176	0.052916	0.071865	0.061358
3	R^2	0.991207	0.98851	0.991149	0.996525	0.990155
	X^2	0.000811	0.001194	0.000859	0.000345	0.001093
	RMSE	0.028069	0.033987	0.028783	0.018926	0.032069
4	R^2	0.978245	0.964543	0.974646	0.973979	0.975551
	X^2	0.002008	0.003688	0.002462	0.002789	0.002715
	RMSE	0.044163	0.059739	0.048729	0.051823	0.050551
5	R^2	0.990822	0.985891	0.990085	0.995352	0.98858
	X^2	0.000847	0.001466	0.000963	0.000498	0.001268
	RMSE	0.028678	0.037663	0.030467	0.021889	0.03454

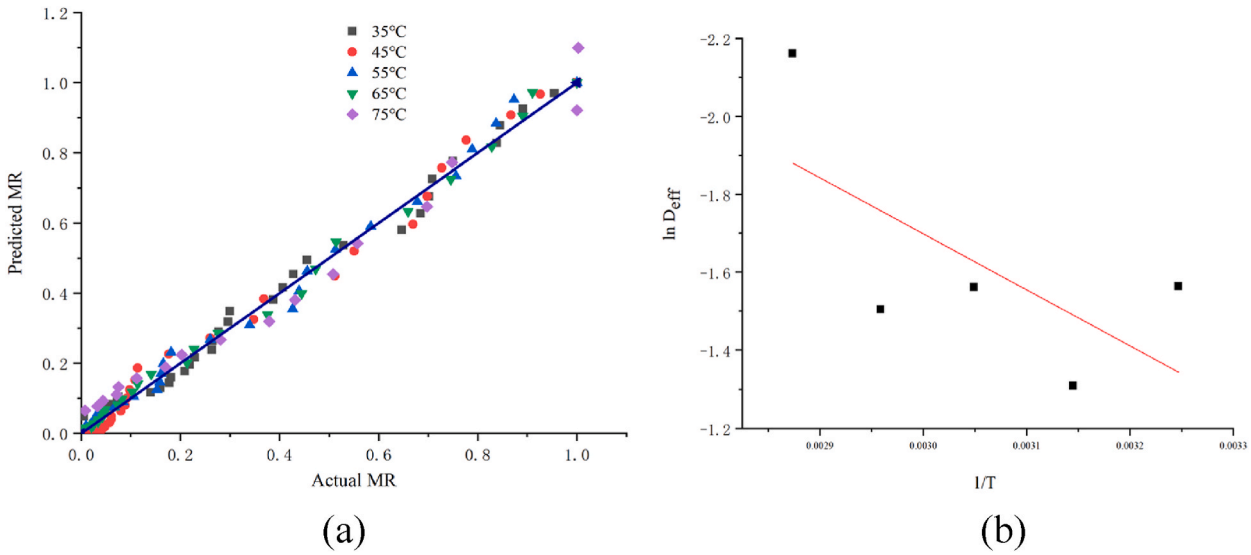

Fig. 2. (a) The predicted MR by the Overhults model vs Actual MR, (b) the relationship between effective ln Deff and temperature.

The primary explanation for this is that the textural features of a product correlate with its sensory appeal. We used SEM to analyze the microstructure of FA subjected to a range of drying conditions (Fig. 3). The morphology of epidermal cells was visibly condensed in the dried FA, but overall, we observed that the samples dried using various settings had comparable appearance and homogeneous textural properties.

As shown in Fig. 3, condensed stomata were dispersed on the surface. For the thin-layer dried samples at 35 °C, the surface shrank somewhat in texture with various drying settings, and the stomata were dispersed. For samples dried at 45 °C and 55 °C, the epidermal shrinkage was greater but the stomata were more evenly spaced over the surface. After drying at 65 °C and 75 °C, the FA samples displayed remarkable epidermal wrinkling, and the outer wall additionally developed arched longitudinal warts. At the same temperatures, the FA's keratin cords were radially organized into a number of bundles, each of which had three to five short keratin cord-like structures. The FA keratin was hemispherically elevated after being subjected to drying at 45 °C and 55 °C, and the texture of the keratin layer was circularly elevated, homogeneous in size, and poorly defined. The ultimate water content may have been lost during drying, which would explain why the membrane structure of dried hedgehog shells changed.

3.3. Volatile contents derived from FA under different drying conditions

As distinctive traits that are exclusive to particular species, odor difference markers have been employed as a basis for characterization. In this work, suitable conditions for gas chromatographic (GC) separation of volatile components were developed by methodically adjusting the temperature gradient. This analysis was undertaken to shed light on the composition of the aroma compounds that give FA its distinctive odor, after exposure to various hot air drying temperatures. As shown by the satisfactory distribution of peak morphologies in Fig. 4, the separation of volatile bioactive components was achieved using an MXT-5 capillary column,

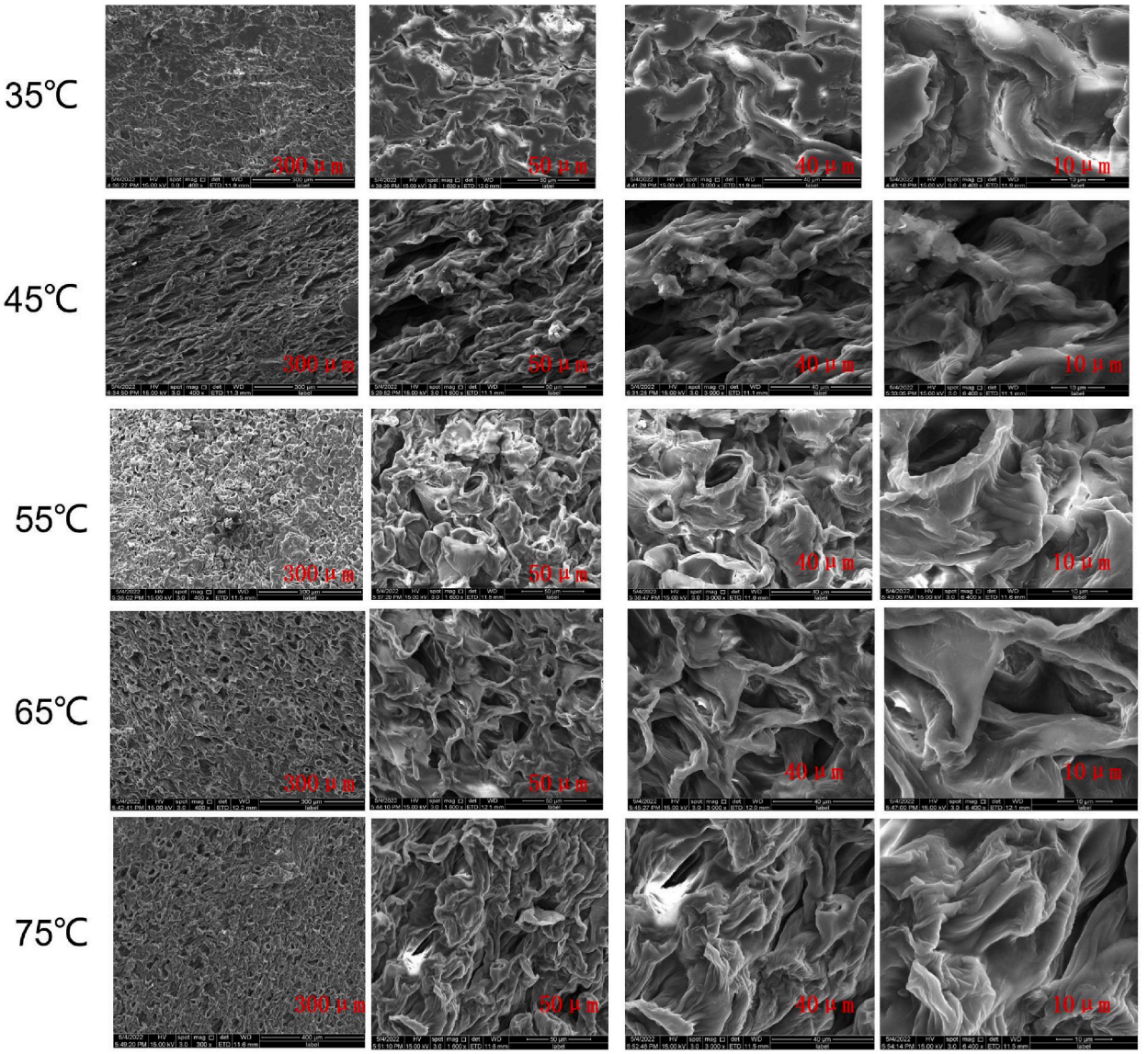

Fig. 3. Scanning electron microscopy results of the FA at different magnifications and temperatures.

thereby allowing us to obtain odor profiles of FA samples dried at various temperatures. Mass spectrometry was used to characterize the peaks, and the identity of each compound was deduced using information gathered from the automated mass spectrometry system, retention times, and pertinent literature. The results are displayed in Table 4. During analysis, each sample was normalized to the maximum peak area of 100% for each component peak based on the results of the electronic nose analysis, and comparative analysis of FA samples dried at different temperatures was carried out using Origin 2021b 64Bit.

The essential details of each volatile component, and their presence in the FA samples, were determined by calculating the Kovats retention indices for two columns for each peak and comparing them with the AroChemBase database, as shown in Table 4. Based on this approach, the principal odor components identified for FA were 1-methyl-4-isopropenyl-1-cylohexene, limonene, terpinolene (δ-terpinene), and acetoin, followed by olefins and esters, then other odorants.

Previous work has established that monoterpenes, sesquiterpenes, and aliphatic compounds—together with other ingredients—-make up the majority of the volatile oil of FA [2], which contains numerous compounds with reported antibacterial [27] and anti-cancer [28] properties. Here, it is important to note that the number of bioactive compounds was found to change dramatically with drying temperature. According to He [29], the major component of the volatile oil of FA is limonene, at 43.1% [30]. Through water diffusion, higher drying temperatures may promote the release of volatile compounds from the matrix of leaf cells. Consequently, more limonene was released from FA as the drying temperature increased, although at the highest temperatures, this trend was somewhat reversed. This could be due to the presence of alkene functionality that makes limonene prone to oxidation in hot air.

The results of this study have helped to clarify the differences in volatile oil profile for FA dried at different temperatures, which will

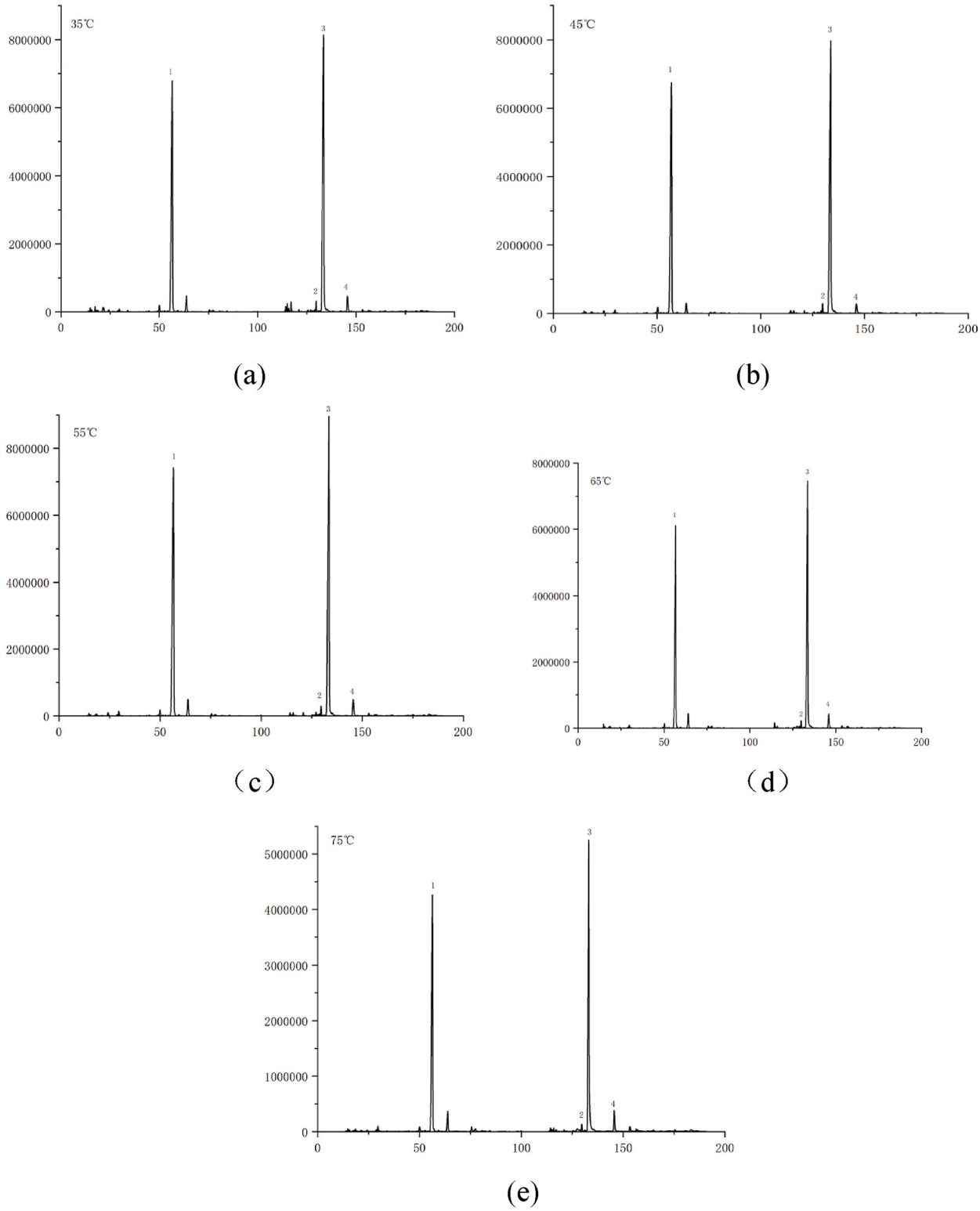

Fig. 4. Total ion chromatogram of volatile oil component Heracles Neo ultra-fast gas-phase electronic nose technology of Fructus aurantii. (a) Fructus aurantii volatile oil after drying at 35 °C, (b) Fructus aurantiai volatile oil after drying at 45 °C, (c) Fructus aurantia volatile oil after drying at 55 °C, (d) Fructus aurantii volatile oil after drying at 65 °C, (e) Fructus aurantii volatile oil after drying at 75 °C.

Table 4
Possible compounds and sensory description information in *Citrus aurantium*L.

No.	MXT-5		MXT-1701		Peak area					Compound	Formula	CAS	Sensory descriptive
	t(R)/min	RI	t(R)/min	RI	35 °C	45 °C	55 °C	65 °C	75 °C				
1	13.96	472	13.82	568	0.22	0.27	0.18	0.16	0.14	ethanol	C_2H_6O	64-17-5	Alcohol; ethanol; spicy; strong; sweet;
2	14.77	494	14.27	583	1.07	0.68	0.78	1.23	0.58	Propanal	C_3H_6O	123-38-6	Acetaldehyde; Cocoa; Earthy; Atmospheric; Nutty; Plastic; Pungent; Solvent
3	24.2	708	20.88	844	0.56	0.88	1.08	0.24	0.32	Acetoin	$C_4H_8O_2$	513-86-0	Butter; Coffee; Creamy; Dairy; Fat; Creamy; Sweet; Woody
4	49.93	990	29.59	1010	2.21	2.11	1.80	1.93	1.60	Myrcene	$C_{10}H_{16}$	123-35-3	Fragrance oil; Fruit; Geranium; Lemon; Metal; Musty; Plastic; Pleasant; Resin; Soap; Spicy; Sweet;
5	51.34	1002	30.82	1027	0.23	0.26	0.28	0.25	0.24	1,3,5-trimethylbenzene	C_9H_{12}	108-67-8	Aromatic; herbal
6	52.64	1013	31.22	1032	0.34	0.24	0.22	0.28	0.18	1-Methyl-4-isopropenyl-1-cyclohexene	$C_{10}H_{16}$	138-86-3	Orange; Atmosphere; Fruit; Green; Lemon; Licorice; Orange; Pleasant
7	56.49	1043	33.47	1061	74.12	82.13	84.18	81.51	78.38	Limonene	$C_{10}H_{16}$	5989-27-5	Orange; fruit; mint flavor; orange; peel flavored
8	60.98	1079	38.12	1118	0.06	0.07	0.07	0.11	0.14	terpinolene	$C_{10}H_{16}$	586-62-9	orange; fresh; fruit; herbal; pine; plastic; sweet; woody
9	63.75	1100	45.49	1196	5.77	3.7292	7.45	5.27	5.05	2-nonanol	$C_9H_{20}O$	628-99-9	cheese; orange; creamy; cucumber; fruit; green; orange; solvent; waxy
10	75.48	1189	53.27	1270	0.70	0.45	0.68	0.89	0.83	Butyl hexanoate	$C_{10}H_{20}O_2$	626-82-4	Berries; Fruit; Pineapple;

affect the composition of medicinal preparations. For example, the volatile oil of FA had the highest level of limonene (84.2%) when dried at 55 °C, and the lowest limonene content (74.1%) when dried at 35 °C, using peak area and temperature is shown the heat map in Fig. 5. As the temperature was raised, the levels of ethanol, myrcene, and 1-methyl-4-isopropenyl-1-cyclohexene all exhibited a decreasing trend (Table 4). This may be caused by sensitivity to heat, since the aforementioned compounds could potentially be harmed or altered when the drying temperature is too high or the drying speed is too rapid. In addition to limonene, the amount of 2-nonanol and acetoin was also greatest in the volatile oil of FA dried at 55 °C, as shown in Fig. 6.

3.4. *Effect of drying conditions on the flavor attributes of dried FA*

A graphical discriminant model was built using Alpha Soft 17.0, then discriminant factorial analysis (DFA) was carried out for the FA samples (Fig. 7a and b). Close to 100% of the explanatory power of the PCA model (99.927% for principal component 1, 0.04218% for principal component 2, and 0.01756% for principal component 3) was accounted for by using these three components as inputs for DFA. As shown in the PCA and DFA model plots, the characteristics of FA dried by hot air at various temperatures differed considerably. The distribution areas for all five temperatures were concentrated and obviously distinguishable, and they could be clearly clustered into five categories. Thus, the results of the PCA and DFA analyses generally matched those for fingerprint identification. The odor fingerprint could successfully distinguish and identify FA batches dried at different temperatures, and the enrichment and dispersion of certain odor molecules discerned using electronic nose analysis (Fig. 7c) revealed that 10 components were connected to odor.

4. Conclusion

The amount of fundamental research on the drying of aromatic herbs is quite minimal, both domestically and internationally. This

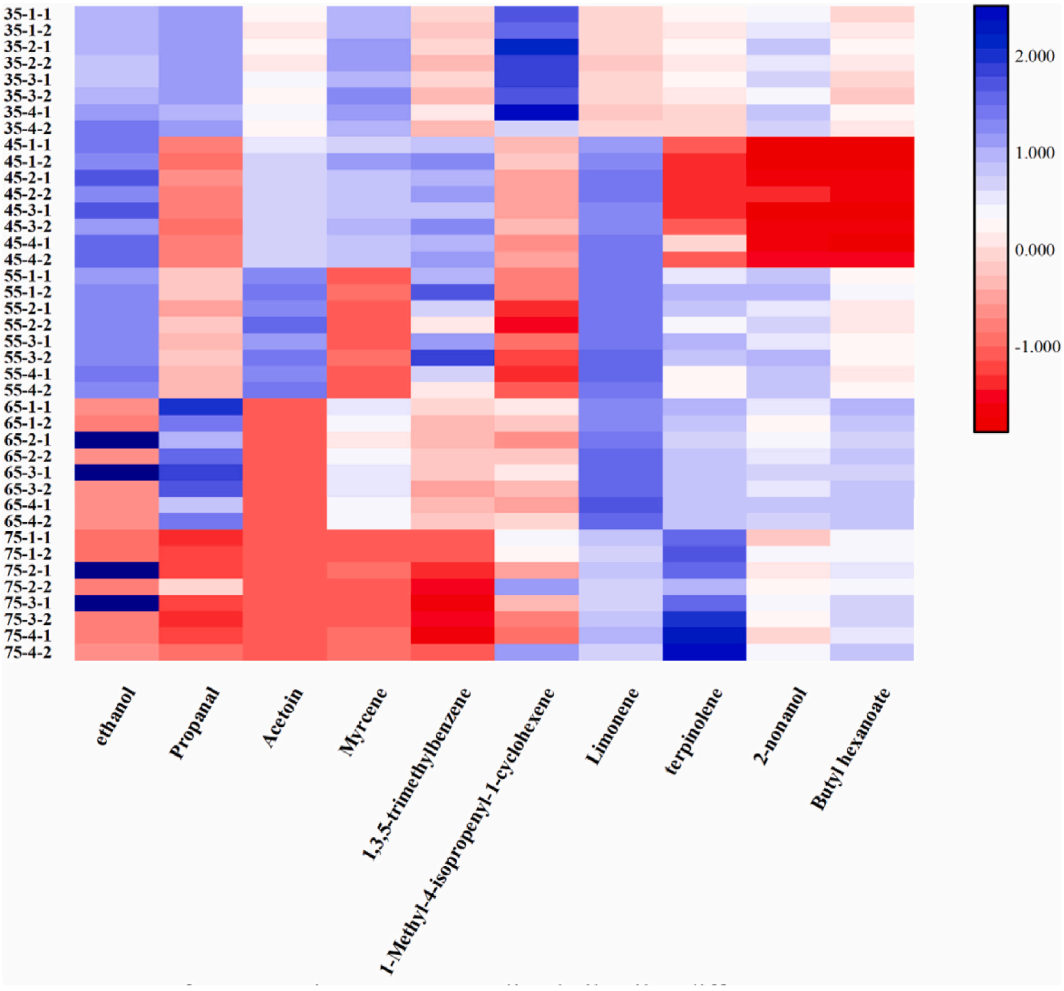

Fig. 5. Heatmap of components in Fructus aurantii volatile oil at different temperature.

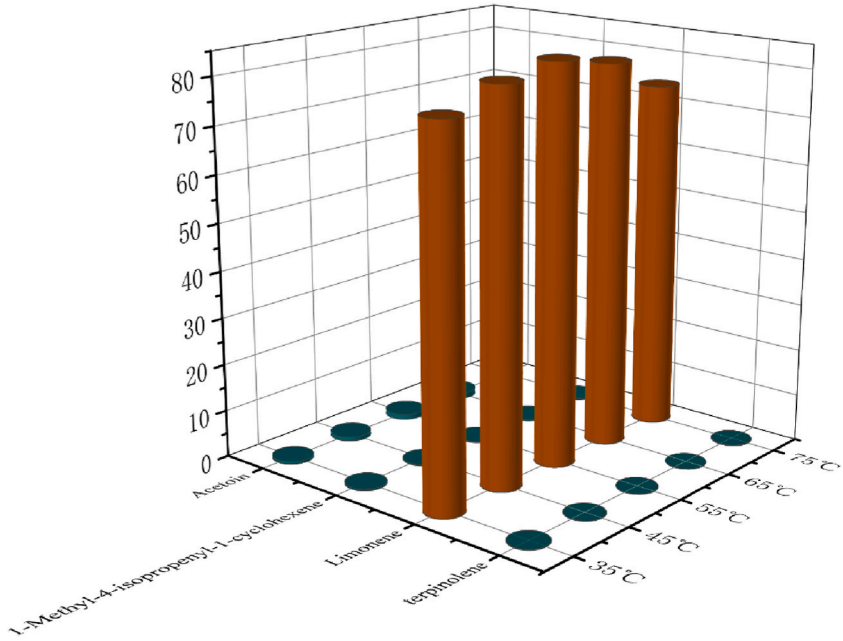

Fig. 6. Contents of four common components in Fructus Aurantii volatile oil at different temperature.

leads to increased reliance on practical experience and repetitive trial and error approaches to determine critical drying parameters for particular plants [31]. There are few explanations, simulations, and quantitative studies of the intricate changes that occur when drying herbs.

The parameters derived using the thin-layer Overhults model suggested that among those considered, this model can most accurately represent the drying of FA. Our findings also indicated that FA dried at 55 °C had the highest total content of volatile components. It is presumed that this is because oxidation or enzymatic reactions took place during drying, under the influence of external factors such as temperature, humidity, and air (oxygen). Therefore, some components in FA could have been converted into volatile compounds after drying. This suggestion is supported by literature reviews [32,33]. Taken together, electronic nose measurements and analysis of the drying curves revealed that this 55 °C was the ideal drying temperature, because it not only shortened the drying cycle and cut costs, but also had little impact on the volatile oil composition, ensuring quality was maintained.

The purpose of this investigation was to combine mathematical modeling with experimental observations of changes in moisture and volatile compound content during drying of FA. By combining theory and practice, we aimed to solve the key problems in the production and processing of FA, and to provide new insights to help address the quality conundrum.

Institutional review board statement

Not applicable.

Informed consent statement

Not applicable.

Author contribution statement

Tingting Bai: Conceived and designed the experiments; Performed the experiments; Analyzed and interpreted the data; Wrote the paper.

Jinlian Zhang: Conceived and designed the experiments; Contributed reagents, materials, analysis tools or data.

Quan Wan, Tao Zhang: Performed the experiments; Analyzed and interpreted the data.

Yating Xie, Min Huang: Performed the experiments.

Rui Ke, Xiangbao Liu: Contributed reagents, materials, analysis tools or data.

Funding statement

This work was supported by National Natural Science Foundation of China, (NO. 82060724, NO. 81560651), the Jiangxi Provincial Key R&D Program (NO. 20192BBG70073), the Jiangxi Provincial Batch Standardization Project (NO. 2021B01, 2021B02).

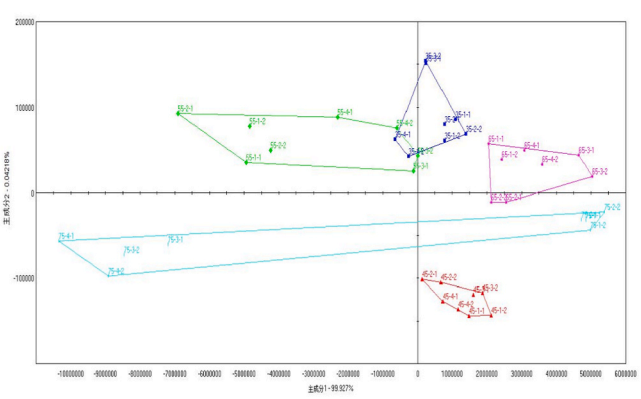

(a)

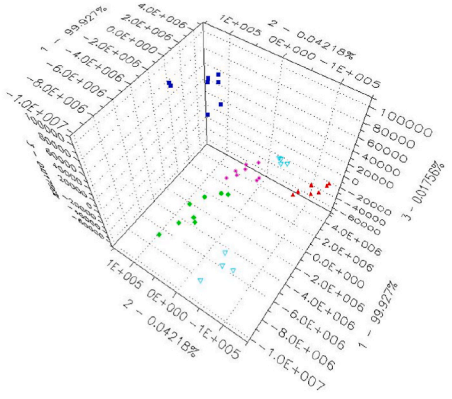

(b)

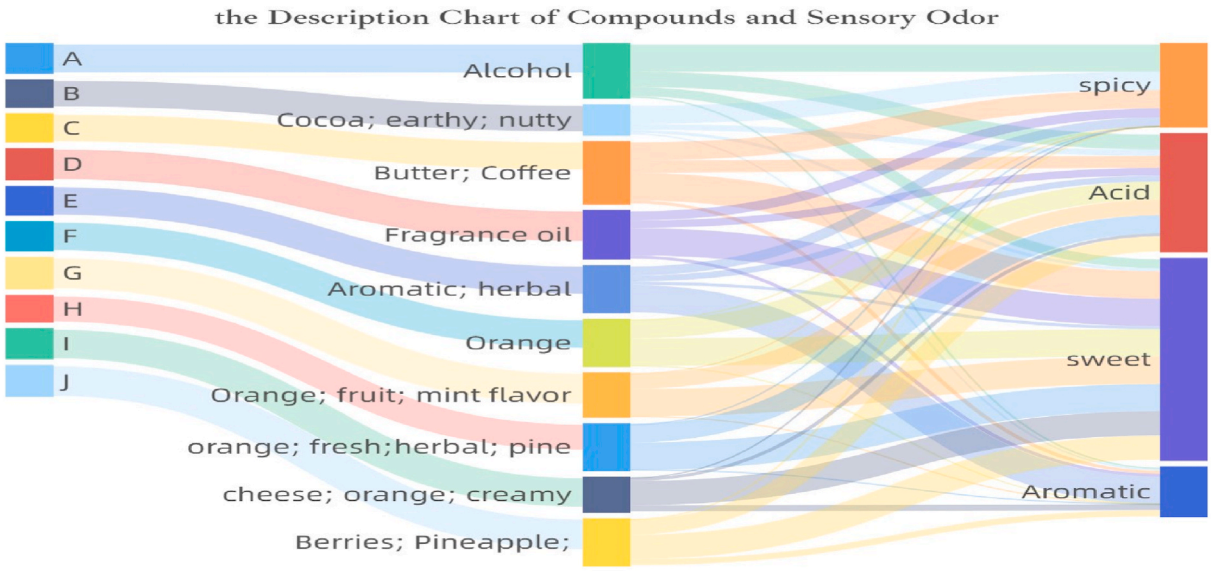

(c)

Fig. 7. (a, b) Cluster analysis chart of Fructus aurantii, (c) the graph of compounds and sensory odor, in the figure c, A = ethanol, B=Propanal, C=Acetoin, D = Myrcene, E = 1,3,5-trimethylbenzene, F = 1-Methyl-4-isopropenyl-1-cyclohexene, G = Limonene, H = terpinolene, I = 2-nonanol, J = Butyl hexanoate.

Data availability statement

Data included in article/supplementary material/referenced in article.

Declaration of interest's statement

The authors declare no conflict of interest.

Acknowledgments

The authors thank J.L. Zhang for assistance in designing the article and for grant support.

Appendix A. Supplementary data

Supplementary data to this article can be found online at https://doi.org/10.1016/j.heliyon.2023.e15554.

References

[1] National Pharmacopoeia Committee, Pharmacopoeia of the People's Republic of China. Part I. Beijing, Chin. Med. Sci.Press, 2020, p. 6.
[2] Jinlian zhang, Minggui Liu, Lingyun Zhong, et al., Optimization of extraction process of volatile oil from Fructus aurantii and analysis of its chemical components by GC-MS, Chin. J. Exp. Tradit. Med. Formulae 19 (2016) 27–31.
[3] Jianye Teng, Screening and mechanism of action mechanism of the chemical substance group of Fructus aurantii for promoting gastric motility, Liaoning Univ. Tradit. Chin. Med. (2011).
[4] Jinlian zhang, Minggui Liu, Dongmei Yan, et al., Acute toxicity study and GC-MS component analysis of volatile oil in raw decoction pieces of Fructus aurantii by Pharmacopoeia method and Zhangbang method, China J. Chin. Mater. Med. 33 (2) (2018) 689–693.
[5] Wei Xu, Yi Zhao, et al., New technology of low-temperature adsorption drying of Chinese herbal medicines containing volatile oil, Chin. Tradit. Pat. Med. 27 (10) (2005) 1135.
[6] Yaokun Xiong, Yeting Zhou, Xinliang Liu, et al., GC-MS combined with principal component analysis to compare the differences in chemical composition of volatile oils of Patchouli before and after drying, Guid. J. Trad. Chin. Med. Pharm. 25 (3) (2019) 83.
[7] Yiping Li, Yanlong Hong, et al., A study on the quantitative transfer of volatile components in clinical preparations-taking an example of Mentha haplocalyx, Chin. J. Tradit. Chin. Med. Pharm. 46 (15) (2021) 3780.
[8] Xiaoli Liu, Fang Wang, Xiaoying Huang, et al., Based on partial least squares method and hydrophilic-lipophilic balance value to explore the material basis of Angelica volatile oil emulsification, Chin. J. Tradit. Chin. Med. Pharm. 46 (14) (2021) 3583.
[9] Hongmei Yang, Chaojie Chen, Xuanrui Zhang, et al., Study on the correlation between the degree of Angelica mildew and the change of coumarin content, Guangzhou Chem. Ind. 47 (23) (2019) 87.
[10] Yingying Sang, Guoyan Zhou, et al., Research progress on drying technology of Chinese medicinal materials, Chin. Tradit. Pat. Med. 32 (12) (2010) 2140.
[11] Seyed-Hassan Miraei Ashtiani, Mahta Rafiee, Mina Mohebi Morad, Cold plasma pretreatment improves the quality and nutritional value of ultrasound-assisted convective drying: the case of goldenberry, Dry. Technol. 40 (8) (2022) 1639–1657, https://doi.org/10.1080/07373937.2019.1670205.
[12] National Pharmacopoeia Commission, Pharmacopoeia of the People's Republic of China. Part IV, Chin. Med. Sci Press, Beijing, 2020, p. 233.
[13] Li Yu, Jingwen Gong, Tulin Lu, et al., Rapid gas-phase electronic nose combined with artificial neural network for rapid identification of three Schisandra decoction pieces and research on odor difference markers, J. Chin. Med. Mater. 53 (5) (2022) 1303–1312.
[14] Jinlian Zhang, Study on the mechanism of slow-drying processing of fengyan tablets and citrus Fructus, Hubei Univ. Tradit. Chin. Med. (2018).
[15] Ashtiani SeyedHassanMiraei, MinaMohebiMorad MahtaRafiee, MehdiKhojastehpour, Impact of gliding arc plasma pretreatment on drying efficiency and physicochemical properties of grape, Innov. food. Sci. Emerg. Technol. (63) (2020), 102381, https://doi.org/10.1016/j.ifset.2020.102381.
[16] Seyed-Hassan Miraei Ashtiani, Alireza Salarikia, Mahmood Reza Golzarian, Analyzing drying characteristics and modeling of thin layers of peppermint leaves under hot-air and infrared treatments, Inf. Process. Agric. 4 (2017) 128–139, https://doi.org/10.1016/j.inpa.2017.03.001.
[17] Bobby Shekarau Luka, Taitiya Kenneth Yuguda, Meriem Adnouni, et al., Drying temperature-dependent profile of bioactive compounds and prediction of antioxidant capacity of cashew apple pomace using coupled Gaussian Process Regression and Support Vector Regression (GPR–SVR) model, Heliyon 8 (9) (2022), e10461, https://doi.org/10.1016/j.heliyon.2022.e10461.
[18] John O. Ojediran, Clinton E. Okonkwo, Abiola F. Olaniran, et al., Hot air convective drying of hog plum fruit (Spondias mombin): effects of physical and edibleoil-aided chemical pretreatments on drying and quality characteristics, Heliyon 7 (2021), e08312, https://doi.org/10.1016/j.heliyon.2021.e08312.
[19] Khuthadzo Mugodo, Tilahun S. Workneh, et al., The kinetics of thin-layer drying and modelling for mango slices and the influence of differing hot-air drying methods on quality, Heliyon 7 (6) (2021), e07182, https://doi.org/10.1016/j.heliyon.2021.e07182.
[20] K.J. Chua, A.S. Mujumdar, S.K. Chou, M.N.A. Hawlader, J.C. Ho, Convective drying of banana, guava and potato pieces: effect of cyclical variations of air temperature on drying kinetics and color change, Dry. Technol. 18 (2000) 907–936, https://doi.org/10.1080/07373930008917744.
[21] M. Torki-Harchegani, M. Ghasemi-Varnamkhasti, D. Ghanbarian, M. Sadeghi, M. Tohidi, Dehydration characteristics and mathematical modelling of lemon slices drying undergoing oven treatment, Heat Mass Tran. 52 (2008) 281–289.
[22] M. Basavaraj, G.P. Kumar, B. Reddy, et al., Determination of drying rate and moisture ratio of fig fruit (Ficus carica L.) by thin layer hot air drying method, J. Food Sci. Technol. 45 (2008) 94–96.
[23] R.A. Chayjan, K. Salari, H. Barikloo, et al., Modelling moisture diffusivity of pomegranate seed cultivars underfixed, semi and fiuidized bed using mathematical and neural network methods, Acta Sci. Pol. Tech. Aliment 11 (2012) 131–148.
[24] K.O. Falade, O.J. Solademi, et al., Modelling of air drying of fresh and blanched sweet potato slices, Int. J. Food Sci. Technol. 45 (2010) 278–288, https://doi.org/10.1111/j.1365-2621.2009.02133.x.
[25] S.J. Kowalski, J. Szadzin′ ska, et al., Kinetics and quality aspects of beetroots dried in non-stationary conditions, Dry. Technol. 32 (2014) 1310–1318, https://doi.org/10.1080/07373937.2014.915555.
[26] Mingyue Xu, The effect of drying conditions on the chemical composition of citrus peel, Shanghai. Ocean. Univ. (2016).
[27] Hui Liang, Shaohua Liu, Jian Ouyang, et al., Analysis of chemical constituents and antibacterial activity of volatile oil from Fructus Aurantii, J. Anhui. Agric. Sci. 45 (11) (2017) 111–113, https://doi.org/10.1186/s12906-021-03285-3.
[28] Na Xing, Zunpeng Shu, Bingqing Xu, et al., Gas chromatography-mass spectrometry analysis and antitumor activity of essential oils from Fructus aurantii from different origins, Inf.Tradit.Chin.Med. 32 (5) (2015) 1–6.
[29] Yingjie He, Construction and Activity Analysis of the Fingerprints of the Active Components of Fructus Fructus Aurantii, Hunan. Agric. Univ., Changsha, 2018.
[30] Hui Wang, Guoyue Zhong, Shouwen Zhang, et al., Research progress on chemical constituents and pharmacological effects of Fructus aurantii and its predictive analysis of quality markers, China J. Chin. Mater. Med. (2022) 1–22.
[31] Huiling Guo, Mengtian Xu, Yaokun Xiong, et al., Study on the drying kinetics of Atractylodes Rhizoma by hot air and the change law of its volatile components, China J. Chin. Mater. Med. 47 (4) (2022) 922–930.
[32] Xiaoxia Yan, Yanlian Qiu, Maoyuan Wang, et al., GC-MS analysis of volatile oil components in Yizhi fruit before and after drying, Chin Cond. 45 (12) (2020) 138.
[33] Liang Chen, Yaning Hu, et al., GC-MS analysis of essential oil components of rosemary leaves before and after drying, Jiangsu Agric. Sci. 47 (24) (2019) 171.
[34] Aijin Yang, Jinfeng Bi, Qingdian Han, et al., Effect of process parameters on water diffusion during puffing and drying process of apples with variable temperature and pressure difference, J. Nucl. Agric. Sci. 27 (4) (2013) 443–451.
[35] Fenghe Wang, Yechun Ding, Pengxiao Chen, et al., Hot-air drying kinetics of camellia seeds, Trans. Chin. Soc. Agric. Mach. 49 (S1) (2018) 426–432.
[36] M. Barrozo, D. Sartori, J.T. Freire, A study of the statistical discrimination of the drying kinetics equations, Food Bioprod. Process. 82 (3) (2004) 219.
[37] He Gao, Jianyong Yi, Jinfeng Bi, et al., Drying characteristics of papaya with medium and short wave infrared, Food Sci. (N. Y.) 36 (7) (2015) 30–35.
[38] Miao Liang, Pei Hou, Changtong Lu, et al., The effect of Lysimachia chin- ensis polysaccharides on the drying kinetics characteristics of sheet tobacco, J. Yunnan Agric. Univ. 34 (1) (2019) 70–77.